Journal of Radiological Protection

Official journal of the Society for Radiological Protection

PAPER • OPEN ACCESS

Validation of a novel radiation mapping platform for the reduction of operator-induced shielding effects

To cite this article: P G Martin *et al* 2018 *J. Radiol. Prot.* **38** 1097

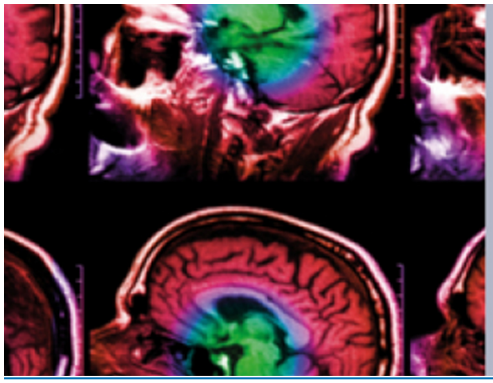

OPEN ACCESS
IOP Publishing | Society for Radiological Protection Journal of Radiological Protection
J. Radiol. Prot. **38** (2018) 1097–1110 (14pp) https://doi.org/10.1088/1361-6498/aad5f2

Validation of a novel radiation mapping platform for the reduction of operator-induced shielding effects

P G Martin[1], C Hutson[1], L Payne[1], D Connor[1], O D Payton[1], Y Yamashiki[2] and T B Scott[1]

[1] Interface Analysis Centre, HH Wills Physics Laboratory, University of Bristol, Bristol, BS8 1TL, United Kingdom
[2] Graduate School of Advanced Integrated Studies in Human Survivability, Kyoto University, 606-8501, Japan

E-mail: peter.martin@bristol.ac.uk

Received 26 March 2018, revised 23 July 2018
Accepted for publication 26 July 2018
Published 14 August 2018

Abstract

With extensive remediation currently ongoing because of the Fukushima Daiichi Nuclear Power Plant accident, there exists the even greater need to provide a system with which the distribution of radiation (specifically radiocesium) can be rapidly determined across extensive areas, yet at high (metre or sub-metre) spatial resolutions. Although a range of potential survey methods have been utilised (e.g. fixed-wing aircraft, helicopter, vehicular and more-recently unmanned aerial vehicle) to characterise the distribution of radiological contamination, ground-based (on-foot) methods that employ human operatives to traverse sites of interest remains one of the primary methods through which to perform routine radiological site surveys. Through the application of a newly-developed platform carried as a backpack-contained unit, it was possible to map sites at twice the rate previously possible—reducing not only the exposure time of the operator to ionising radiation, but also dramatically reducing the level of radiation attenuation (introduced by the operator) onto the detector. Like magnetometry platforms used during geological ore prospecting, this system was similarly boom-based, extending sideways away from the central operator. While conventional radiological survey platforms require a correction be performed on the data to account for the carrier (aircraft, vehicle or human) interception and attenuation incident radiation—this system is shown to not require such a retrospective correction.

Supplementary material for this article is available online

Keywords: Fukushima, FDNPP, radiological mapping, bodily attenuation, site-wide monitoring, contamination characterisation

(Some figures may appear in colour only in the online journal)

1. Introduction

Radiological surveys of sites of interest are occurring worldwide. These investigations are typically in response to anthropogenic pollution; as is the case with current remediation activities across the extensively contaminated Fukushima Prefecture [1], or associated with nuclear site remediation—forming a core part of a sites eventual post-operational clean-out [2, 3]. Owing to factors including, but not limited to; the time available, spatial-resolution required, potential radionuclides of interest, detector type and site/regional terrane/topography encountered alongside the overall accessibility of the site—a range of different 'carrier' options have been employed to perform these radiological surveys.

The greatest site coverage (at the compromise of attaining the lowest spatial-resolution results), is achieved via airborne sensing using manned helicopters or fixed-wing aircraft. These systems typically operate at survey altitudes of 120–700 m, at velocities of greater than 50 ms^{-1}, and subsequently produce on-ground pixel diameters greater than 500 m [4, 5]. Surveys of such a rapidly-deployable nature are typically conducted in the immediate aftermath of a large-scale nuclear release event [5, 6], or conversely, for the regional study of naturally-occurring radioactivity [7]. The application and calibration of these high-altitude gamma-ray spectrometry survey methods, applied to both exploratory (mineralogical) as well as emergency response scenarios, is detailed extensively in the 1991 IAEA Technical Report on the subject [8]. The results of a multi-national exercise that sought to develop standards for nuclear emergency monitoring (using helicopter-mounted detectors), are described in the work by Bucher *et al* [9]. The results of this work are characterised by the successful implementation of radiation surveys at altitudes of 100 m and flight velocities of 100 $km\,h^{-1}$—which together contributed to improved spatial (on-ground) resolutions of 250 m. Later work by Guastaldi *et al* [10], using an autogyro to transport the detector during a regional-scale radiometric survey of Elba Island (Italy) served to further enhance not only the spatial-resolution, but also the spectral resolution/peak signal quality.

A further increase in the spatial-resolution attainable using airborne systems has been achieved through the application of low-altitude unmanned aerial vehicles (UAVs)—either miniaturised remote-control helicopters and multi-rotor drones. These platforms have together permitted for the on-ground resolution of aerial surveys to be reduced from hundreds of metres per pixel, to approximately 5 m [11–13], and 1 m per pixel [14, 15] for helicopter and multi-rotor platforms respectively. As a consequence of their versatility and rapid deploy-ability, both system types have been employed extensively in response to the multiple radiological releases resulting from the 2011 Fukushima Daiichi Nuclear Power Plant (FDNPP) accident [11, 12, 15]. Acting fully-autonomously, these systems are advantageous in not exposing those conducting the works to harmful ionising radiation.

Due to the slow velocity at which ground-based surveys are performed (a consequence of the walking pace of the operator) the time required to perform these high-resolution ground-based radiation surveys is the greatest per area coverage of all the aforementioned

techniques. Countering this slow rate of data collection in direct response to the FDNPP accident was the 'crowd-sourced' Safecast platform [16]. This 'distributed' radiological survey utilised a network of hundreds of mobile-phone tethered Geiger–Muller (GM) tube-based systems—each carried by members of the public. These units simultaneously logged their position, activity level and resulting calibrated dose-rate across Fukushima Prefecture [17].

Vehicular-based surveys have also been devised and widely deployed, whereby detector systems typically carried as part of ground-based detection systems (although often using larger volume detectors due to the increased carrier capacity which can be afforded) are mounted onto vehicles and subsequently driven around the region of interest. One example of such a system is the KURAMA-II platform [18, 19]—itself similarly developed as a consequence of the March 2011 FDNPP accident. Using solid-state (NaI) detectors, the suitcase-sized system was installed onto the public bus network that operated across the affected region, as well as on bicycles belonging to members of the public.

As has been quantified in works by other authors [20, 21], it is typical for bodily attenuation of gamma-ray radiation to reduce the recorded values by between 15% and 30%, depending on the energy profile of the incident radiation and the exact bodily proportions/physical attributes of the person. To negate against the effects this shielding has on the accuracy of the results, it has been determined that corrections (to the as-collected data) should be appropriately applied [20], following empirically-derived calibration experiments specific for that detector and/or operator. The same detrimental influence of detector shielding (and associated radiation attenuation) is also experienced during radiological surveys performed using either aircraft and vehicular carrier methods. In each case, a thorough understanding of the shielding geometry surrounding the detector volume is needed for adequate normalisation. To negate against having to perform such shielding corrections associated with foot-based radiological surveys, a new type of telescopic (or boom) based system was developed and is described in this work. Using two identical pole-mounted detectors as part of this novel system, the time taken to perform a routine survey in a radiologically contaminated environment is considerably reduced, therefore resulting in a marked dose-rate reduction for the systems operator over conventional ground-based methods.

2. Experimental

2.1. Mapping system

A schematic of the system designed and implemented in this work is shown in figure 1. Worn on the operators back is a small waterproof backpack in which the systems control electronics are contained. From this backpack, a toughened plastic tube extends out sideways—this serves to hold both scintillator-type radiation detectors and to support the two above detector external GPS antennas. A single unit version of this dual-unit system, with output tailored for visualising on a mobile-phone was previously developed as an educational tool by the authors [22].

In addition to a small lithium polymer (LiPo) battery and associated power regulation electronics, the control electronics consists of two identical sets of circuit-boards, one for each of the systems gamma-ray detectors. Each set of electronics consists of an Arduino™ Mega ADK board (Scarmagno, Italy) onto which an SD-shield is mounted. Incoming data from the multiple streams (position, height and individual incident gamma-ray photon energy) was collated before being written onto a micro-SD card installed on the SD-shield board. The

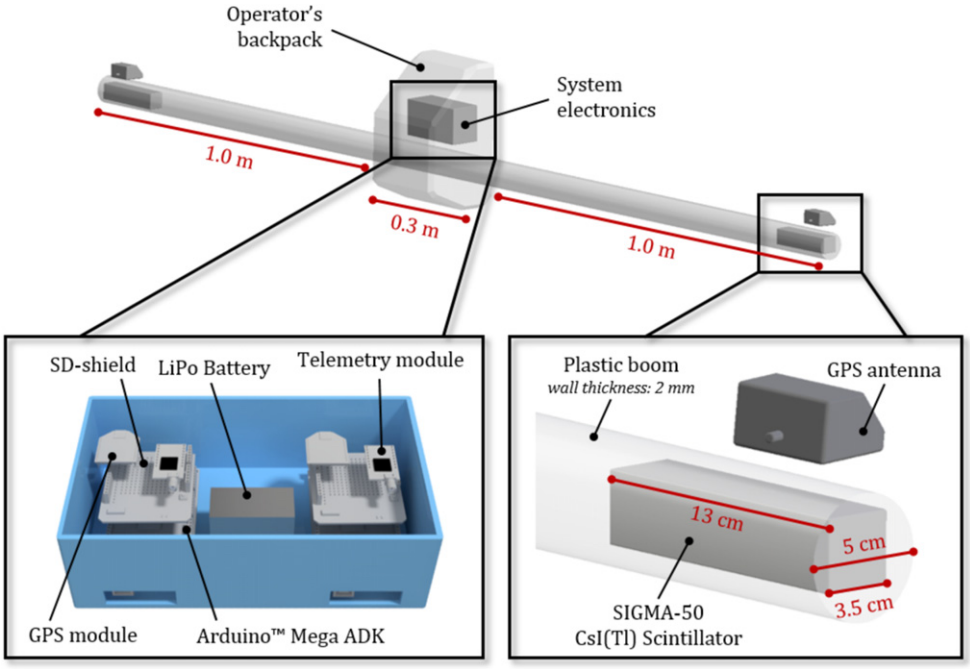

Figure 1. Schematic representation of the radiation mapping platform devised during this study. The system consisted of two Kromek SIGMA-50 CsI(Tl) scintillator detectors each contained within plastic tubing, 1.0 m away from the operator's backpack—which contained the central data collection and processing electronics. External GPS antennas were additionally mounted onto the ends of the plastic piping to provide for an accurate position location for each of the detectors.

position data for each of the detector units was determined using a high-spatial accuracy GPS chip (MTK3339), also contained within the system electronics, as shown in figure 1. The external GPS antennas positioned at either end of the plastic tubing, directly above each of the detectors, recorded the position of these units rather than the GPS chip/central system electronics that was carried by the human operative. To communicate results back to a nearby ground-station, a radio-telemetry module was also installed onto each of the two identical electronic setups. These units transmitted data in near real-time (at two differing radio-frequencies) via a securely encrypted data-link to a dedicated field data laptop.

The toughened plastic tubing selected for this system had an internal diameter of 50 mm, with a wall-thickness of 2 mm, and a total length of 2.3 m end-to-end. This length of tubing was selected for both detectors to exist at a distance of 1 m from the centrally positioned operator (whose width while wearing the backpack was 0.3 m).

For this survey system, two thallium-doped caesium-iodide, CsI(Tl), SIGMA-50 scintillator detectors from Kromek Ltd (Co. Durham, UK) were used. These detectors featured a $25.4 \times 25.4 \times 51.0$ mm crystal of the material (total volume 32.8 cm^3) contained in a 2 mm thick aluminium case alongside the required detector/signal processing electronics. These electronics consisted of a Si photomultiplier tube (Si-PMT) connected to a multi-channel analyser to derive per-channel intensities and, therefore, a gamma-ray spectrum across the units 4096 calibrated energy bins. These detectors possessed an energy range of 50 keV to 1.5 MeV, with a maximum throughput of 5000 counts per second (CPS). This range hence

represented a per-channel gain of 0.36 keV. These properties were imposed by the manufacturer through the detectors pre-configured electronics (e.g. electrical gain and bias) and could hence not be modified by the end-user. A typical spectral resolution of <7.2% full width at half maximum at 662 keV (^{137}Cs) was quoted by the detectors manufacturers. With a total weight of 300 g, these gamma-ray spectrometers are easily incorporated into detection systems such as this.

To achieve the greatest possible sensitivity to the incident radiation emitted from the ground directly below the detector, each of the detectors was placed with the long-axis of the crystal running parallel to the ground surface (figure 1). This orientation (with one of the 25.4 × 25.4 × 51.0 mm crystal faces positioned parallel to the horizontal) for optimum detector sensitivity, was confirmed following detector calibration and analysis, the results of which are shown in figure S1 is available online at stacks.iop.org/JRP/38/1097/mmedia. A count rate increase of between 35% and 89% (dependent upon incident gamma-ray photon energy) was observed when each of the calibration sources was incrementally moved from directly in front (underneath) the SIGMA-50 detector through 90° to the detectors side (and the larger CsI(Tl) crystal face).

An important consideration of airborne radiometric surveys is the 'field of view' or on-ground 'radius of investigation' [23]. This numerical value represents the region/footprint on the ground the detector samples during the survey flight. The value is a function of both the height of the detector as well as the detectors physical aperture to accept incident radiation. To quantify the 'field of view' and therefore the on-ground sampling footprint of the SIGMA-50 detector contained within this boom-based platform, a calibration experiment was undertaken. This calibration was performed by positioning a single 1 MBq ^{137}Cs point-source at a range of positions outwards from a central origin—the same vertical axis on which the SIGMA-50 detector was held at varying heights (0.5–10.0 m) above the ground. Through taking intensity measurements at each source angle/detector separation, the 'radius of investigation' was determined—taken as the value at which 50% of the gamma-ray intensity was recorded when the detector (at the same height) was located directly above the point-source (90° in figure S1). Owing to the strongly-normal distribution of the results ($\sigma^2 = 0.5$), and the absence of formerly-published values for comparison, this value was selected. As expected, this analysis indicated a strongly-positive linear correlation ($r^2 = 0.98$), with a 1:1 relationship between the height of the detector and the on-ground sampling radius, the results of which are shown in figure S2. For a 1 m above-ground detector height, a 1 m 'radius of investigation' (2 m diameter) was apparent. This relationship is consistent with the logic and derivation described in the early work by Pitkin and Duval [24], shown in equation (1), whereby R = the radius of investigation, H = height of detector, and tan θ = detector aperture angle (determined as 45°). The numerical derivation of this rationalisation is detailed in figure S3 and expressed numerically in equation (2) in the supplementary material.

$$R = \tan\theta \times H. \tag{1}$$

An integration time of 60 s at each spatial measurement point was used to ensure a high signal (to noise) quality. The accurate spatial determination of the radiation source, taken here to represent a (mathematically infinite) series of point sources, was important in undertaking a nearest-neighbour correction/deconvolution of the radiometric data to both remove spurious data points as well as locating specific points/regions of interest post-survey—the application of which is detailed in previous works [14, 15].

Control of the detectors and the consolidation of the data arriving from it and the GPS modules was performed using custom-written software produced at the University of Bristol. Post collection, data was downloaded from the systems two micro-SD cards and processed on

additional custom-designed software produced at the University of Bristol. Resulting from the use of gamma-ray spectrometers over the simpler gross-counting method of GM-tubes, the isotopic nature of any contamination can be determined, and the specific source(s), whether naturally-occurring or anthropogenically-derived, consequently attributed.

2.2. Survey site

Resulting from the large-scale decontamination effort that is currently ongoing across the contaminated area to the west of the FDNPP, a considerable volume of radiologically contaminated soil and vegetation is being removed from the surface environment. This waste material is being packed into large high-density plastic bags before being transported off-site to a number of storage facilities that continue to be established across the region [1, 25]. The initial testing and validation of this platform were conducted at one of these waste storage sites in the Kawamata region of Fukushima Prefecture (location: 37° 35′ 30.88 N, 140° 42′ 1.45 E). This site consisted of several hundred of the 1 m^3 black storage bags that are now strongly-associated with the accident and its resultant clean-up. Like many of the countless other sites that exist to house this material (as an interim measure prior to its final long-term storage), this site was still under the final stages of construction and was receiving additional material on a continual basis at the time of the survey. Each bag was stacked to form a cubic-centred packing arrangement.

For the validation survey, the operator traversed backwards and forwards across the site in a north–south grid pattern, walking over and amongst these waste storage bags as they were encountered on their route.

3. Results and discussion

3.1. Detector inter-comparison

With only one of the two detectors transiting over any specific area of the surveyed ground, it was crucial to the performance and results of the system that the boom-mounted gamma-ray spectrometers were recording complementary values when exposed to identical radiation (activity) levels. To ensure this consistency, both in-lab and in-field calibrations were undertaken on both the detectors, and the entire system, respectively. For this calibration, both SIGMA-50 detectors (designated as SIGMA-50 ‘A’ and SIGMA-50 ‘B’) were positioned side-by-side at various positions and exposed to differing activity gamma-emitting radiation sources (^{60}Co and ^{137}Cs). From these results, as would be anticipated from two identical detectors, a strong correlation was observed between the radiation intensity observed by the two gamma-ray spectrometers—with an r-squared value of 0.97 determined when the data was plotted, and a linear regression fit applied. The additional in-field calibration of the detectors within Fukushima Prefecture is subsequently shown in figure 2. For this second calibration, the systems operator traversed a 50 m path northwards pausing with each step (with SIGMA-50 ‘A’ passing over the identified portion of the radiocesium contaminated ground), before turning around and returning southwards to the start position, retracing their steps. This time, however, SIGMA-50 ‘B’ transited over the same portion of contaminated ground. An integration time (data collection period) for each data point was 10 s, representing the time the operator paused after taking each large footstep. From the results presented in figure 2, a similar degree of correlation was witnessed between both detectors—with a mean percentage difference of 2.3% and a standard deviation, σ, of 0.61. This correlation therefore permits for the gamma-ray intensity measurements from both units to be directly compared and used interchangeably.

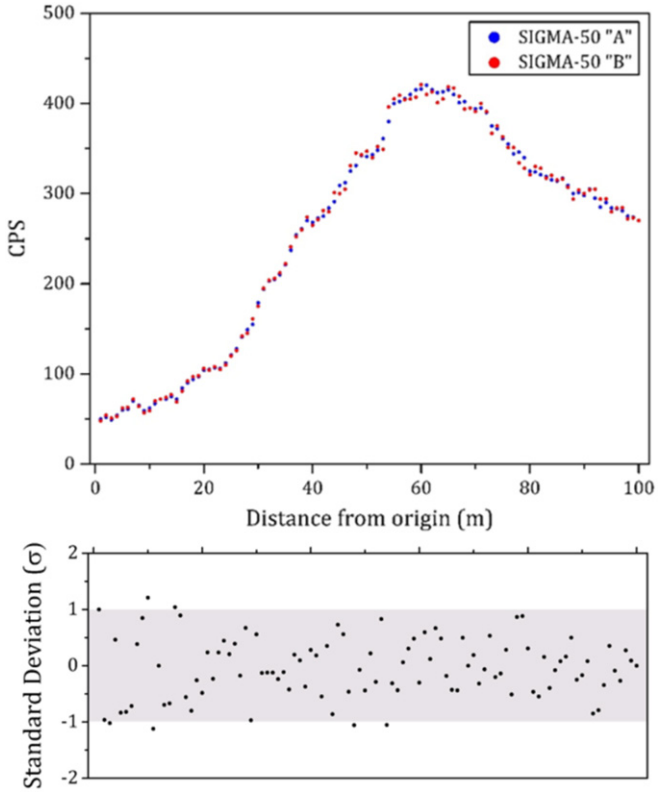

Figure 2. Comparison of both SIGMA-50 CsI(Tl) scintillator detector units traversing a 100 m transect of the contaminated site, with each of the detectors (SIGMA-50 'A' and SIGMA-50 'B') travelling directly over the same portion of ground. A plot detailing the standard deviation (σ) between the two values is additionally shown—with 94% of all values existing within 1σ. An integration time of 30 s per data point (sampling locality) was used.

3.2. GPS responses

As a consequence of both the boom-mounted external GPS aerials being located within such close proximity to one other (2.3 m), an appreciable and undesired amount of radiofrequency (RF) interference is likely to occur. This interference will culminate in potentially erroneous values derived for the systems position. To assess this possible RF-induced degradation of the platforms position, a portion of the radiation survey was analysed in detail. The results of this analysis are shown in figure 3. In this plot, the positions of detectors (SIGMA-50 'A' and SIGMA-50 'B'), as determined by their GPS antennas, are plotted as blue and red data points respectively. The position of the operator, taken as the location lying equidistance between both detector positions, is also plotted (in black). From this data it was observed that the impact of any RF interference on accurately determining the GPS position of both SIGMA-50 detectors was negligible, with none of the points collected during this sub-survey showing 'wandering' that would be expected if such interference were to occur. This was confirmed statistically, with an *r*-squared value of 0.96 yielded when both *X* and *Y* values were subsequently linearly-graphed.

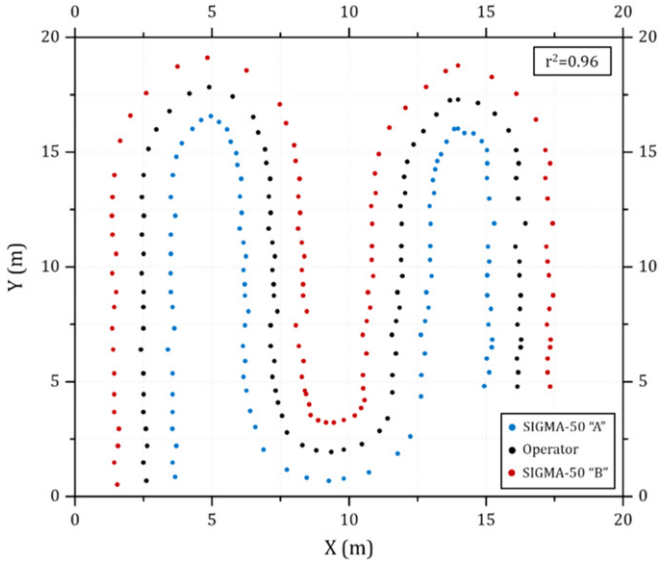

Figure 3. Plot of GPS-derived position recorded by the two GPS receivers positioned above the two Kromek Ltd SIGMA-50 scintillator detectors, located at either end of the plastic 'boom' within which they are contained. The location of the 'operator' is inferred as existing at the midway position (1.15 m) between the two detectors/receivers. A high degree of positional reliability from both GPS units is observed, with 98% of all data points (pairs) occurring within 1 standard deviation (σ).

3.3. Operator attenuation

As formerly mentioned, a core issue and consideration for ground-based (human) radiological surveys is the significant impact that bodily radiation attenuation/detector shielding (by the operator) can have on the measured radiation intensity. With the human body being predominantly constituted of a high water content (approximately 48 $\pm$ 6% and 58 $\pm$ 8% for both women and men respectively [26]) and with water being known to represent a strong absorber/attenuator of gamma-ray radiation [21]—this reduction can potentially be considerable, but difficult to accurately (numerically) quantify.

For this attenuation test; a radiocesium point-source was located at a central position within an area of non-radiologically contaminated ground. The operator of the survey, beginning at 1 m from this source whilst facing the point-source and holding the detector directly in front of them, progressively stepped backwards. Measurements of the activity level (as CPS) were directly recorded across the range of distances. After reaching 6 m from the radioactive source, the operator turned 180°, so to position their back to the source. The operator then progressively moved slowly backwards towards the source—with the raw CPS values similarly recorded against the range of distances from the radiocesium point-source. An integration time of 120 s per measurement was used, with an average CPS value used in the subsequent operator attenuation analysis.

The results of this simplistic attenuation calibration are plotted in figure 4, detailing the CPS measurements in instances of both operator obstructed attenuation and when no such detector shielding occurred. A clear disparity is observed to exist because of the occurrence/positioning of the human body between the source and the detector, with a difference between

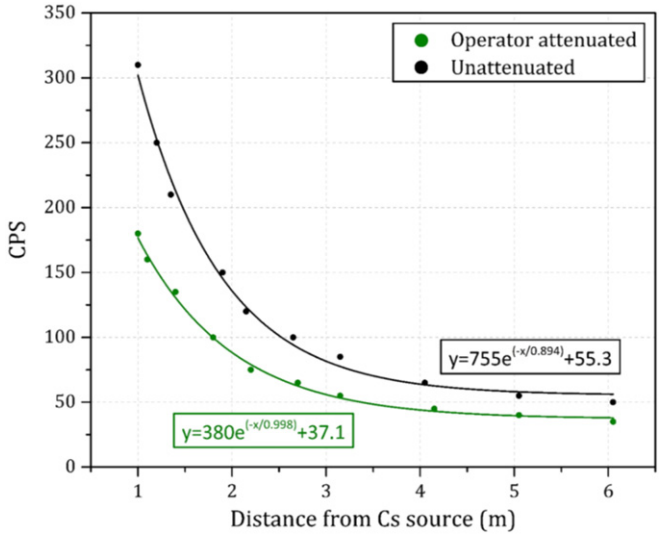

Figure 4. Influence of operator-induced attenuation on measured radioactivity levels, as recorded by a SIGMA-50 scintillator detector using a radiocesium point-source emitter. The equations for the exponential fits applied to both curves is also shown. A per-point integration time of two minutes was used—with the average value derived from these results.

an obscured/unobscured source averaging 35% across the range of distances (1–6 m), used in this calibration.

These results clearly detail the impact of humans on-ground-based surveys, and hence the requirement to eliminate their influence to afford radiation survey results with the highest level of detection accuracy. The installation of the two SIGMA-50 detectors contained inside the toughened plastic tubing represents a methodology to dramatically reduce attenuation effects than if the detector(s) were to otherwise be transported (during the survey) closer to the operator, such as within their backpack or in close proximity to their body.

3.4. Radiation mapping

The results of the radiological survey of the Kawamata waste store using this new dual-unit radiation detection platform are shown in figure 5, alongside an aerial image of the site—generated from numerous composite images. The combination of this new radiation mapping system coupled with aerial photogrammetry of the site is presented in Connor *et al* [27]. From the radiation map, the location of the waste bags towards the northern extent of the site (illustrated graphically in figure 5) is evident due to the elevated levels of radioactivity within the highlighted region. Despite the prior remediation of the site having occurred ahead of the arrival of the waste material, elevated levels of radiation exist across much of the store—a full assessment of this is discussed in the aforementioned works by Connor *et al* (2017). Of note is the elevated CPS activity (over the area immediately to the west of the storage bags—identified as (b) in figure 5) displayed by the north–south trending access road to the west of the site (identified in figure 5), where contamination likely originating from vehicles transporting material to the store has also served to contaminate the track. Further observed is the area of heightened radiological intensity to the south of the store (slightly downslope), arising from the leakage and transport of contamination out of the large storage bags due to the heavy

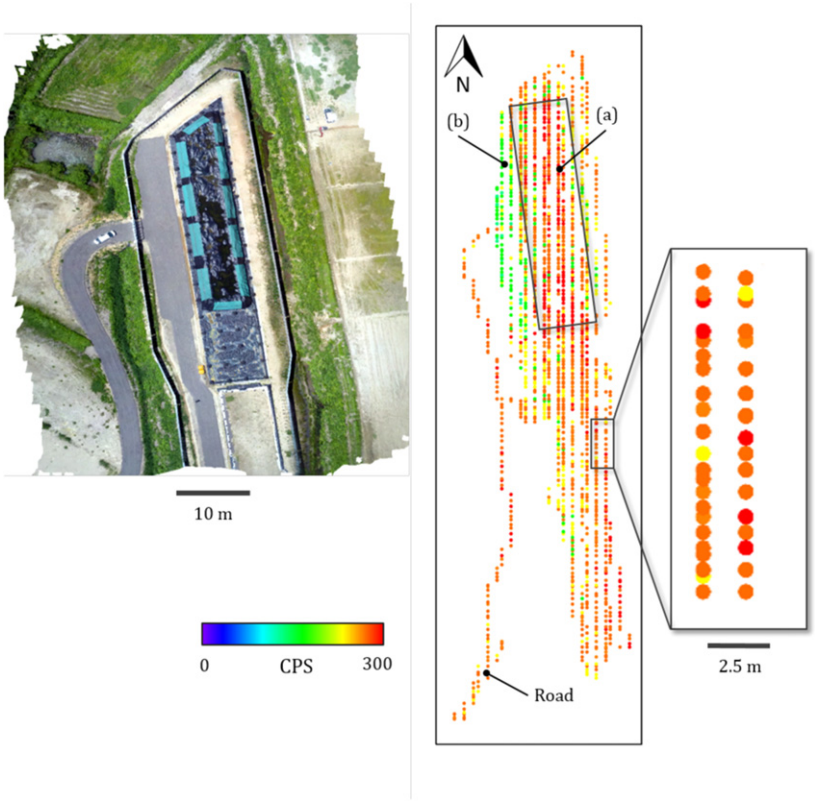

Figure 5. Radiation intensity data obtained across a waste storage site located in the Kawamata Town area of Fukushima Prefecture. A clear 2.3 m separation between each of the lines of parallel data points is observed. Elevated count rates (CPS) are associated with the position on the site at which the bagged contaminated wastes are located. The small number of discrete areas across the site where no measurement data is observed are associated with water-covered areas which represented access limitations during the ground-based survey. The location of the access road to the compound to the west of the site is shown—with steep banks existing on either side of this track making such ground-based surveys difficult to perform. The positions (a) and (b) on the site where gamma-ray spectra were obtained (shown in figure 6) are additionally shown. A composite aerial photograph of the site at the time of the ground survey is shown for reference.

rain associated with the prevailing typhoon-type conditions, characteristic of the region [28]. The regions in figure 5 where no data points exist (concentrated largely over the contaminated waste bags) are associated with positions where the ponding of water made radiological survey access not possible.

Gamma-ray spectra obtained by subsequently placing the SIGMA-50 detector directly in contact with both the waste bags and imported 'virgin' sand for counting periods of 20 min are shown in figures 6(a) and (b), for the wastes and clean sand respectively. As anticipated from the gamma-ray spectra derived from the wastes, the dominant isotope contributions are those of radiocesium (^{134}Cs and ^{137}Cs)—with the emission peaks from the imported sand in contrast showing peaks associated with the U-series decay chain (^{214}Pb and ^{214}Bi) [29]—typical of the felsic lithologies from which they were likely sourced.

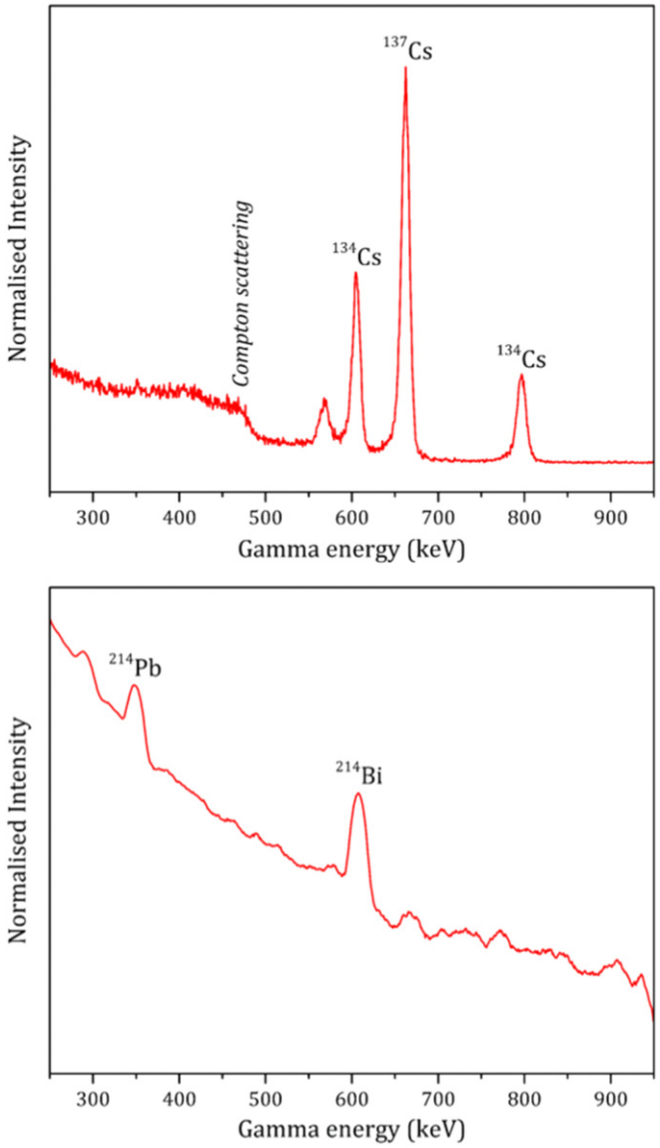

Figure 6. Gamma-ray spectra with the contributing radionuclide emission peaks identified, obtained using the SIGMA-50 scintillator detector (with an acquisition time of 20 min) for; (a) the bagged contaminated waste material, and (b) the imported sand surrounding the site—the locations at which the spectra were obtained are identified in figure 5. The intensity is normalised using the integral of the maximum emission peak.

4. Conclusions and future work

Following extensive calibration and system deployment both in the laboratory as well as within the contaminated Fukushima Prefecture, a novel system with which to accurately map the spatial extent of radiation anomalies over potentially large and topographically-challenging sites has been successfully produced. This newly-developed system—consisting

of two high-sensitivity gamma-ray spectrometer-type radiation detectors, located at opposing ends of a toughened plastic boom (away from the human operative), was not only shown to increase the rate at which data were collected through simply doubling the number of detectors coincidentally deployed, but to also, and more significantly, reduce the influence of operator attenuation on the results of the survey that subsequently require normalisation/correction. Dependent upon the orientation of the operator conducting such a ground-based survey, the shielding induced could represent an attenuation (intensity reduction) of between 0% and 35%—with further complications to such corrections arising when differing persons (with even marginally differing body masses/structures) perform a 'traditional' radiometric ground survey. While other survey options exist for which the human operator is completely removed from the radiological environment, thus eliminating their receipt of any dose, the use of ground-based surveys (although the most time consuming of methods available) provides the greatest on-ground spatial resolution. Through deploying two detectors, the operator experienced dose in performing a survey is effectively halved, therefore representing a significant and highly-favourable radioactive dose reduction. Despite initial concerns relating to the potentially detrimental impact associated with having two closely-located GPS antennas, the results of this work highlighted that the 2.3 m separation used in this work was not an issue in either unit accurately determining its position during a survey.

In this work, the contamination resulting from the FDNPP accident of March 2011 has been mapped at one of the Prefectures numerous interim waste stores—illustrating the contamination arising from likely leakage and vehicular transport. This platform can also be easily employed for the geophysical exploration of radioactive ore minerals over sites of interest following more extensive (wide area) aerial surveys. By using gamma-ray spectrometers as the detectors in this platform instead of the simpler gross-counting Geiger–Muller devices, the isotopic nature of any contamination (or naturally-occurring radioactivity anomaly) can be defined, if spectral analysis over the specific energy windows indictive of certain radionuclides, as discussed previously, were to be conducted rather than the more simplistic use of 'raw' CPS activity as in this work.

Future work will seek to refine the on-ground 'radius of investigation' of the system to attain a reduced source 'footprint' through potential detector collimation or changes to the crystal geometry used. Alongside this refinement, additional work will examine the influence of different compositon detectors on both radiation sensitivity and spectral resolution with a goal to undertake spectral stripping/window analysis to determine specific isotopic contributions.

Acknowledgments

The authors wish to thank the Daiwa Anglo-Japanese Foundation for providing the financial support that enabled the fieldwork expedition to Japan to occur. Thanks are also extended to local officials and members of the public who kindly granted access to the sites across Fukushima Prefecture. Funding for this work was provided by the EPSRC (Grant Reference: EP/K503824/1).

ORCID iDs

P G Martin https://orcid.org/0000-0003-3395-8656

References

[1] Japanese Ministry of the Environment (Government of Japan) 2013 *Decontamination Guidelines* 2nd edn (http://josen.env.go.jp/en/framework/pdf/decontamination_guidelines_2nd.pdf)

[2] Martin P G, Moore J, Fardoulis J S, Payton O D and Scott T B 2016 Radiological assessment on interest areas on the sellafield nuclear site via unmanned aerial vehicle *Remote Sens.* **913** 10

[3] Wilson P D 1996 *The Nuclear Fuel Cycle: From Ore to Wastes* (Oxford: Oxford University Press) https://inis.iaea.org/search/search.aspx?orig_q=RN:28071286 (Accessed: 5 May 2017)

[4] Sanderson D C W, Allyson J D, Tyler A N and Scott E M 1995 *Environmental Applications of Airborne Gamma Spectrometry* (http://iaea.org/inis/collection/NCLCollectionStore/_Public/27/025/27025425.pdf#page=26)

[5] MEXT, US Department of Energy 2011 *Results of the Airborne Monitoring by the Ministry of Education, Culture, Sports, Science and Technology and the US Department of Energy (6th May 2011*

[6] Guss P 2011 *DOE response to the radiological release from the Fukushima Dai-ichi Nuclear Power Plant* (http://hps.ne.uiuc.edu/rets-remp/PastWorkshops/2011/presentations/6C-DOE Response to the Radiological Release from the Fukushima Daiichi Nuclear Power Plant.pdf)

[7] Beamish D 2014 Environmental radioactivity in the UK: the airborne geophysical view of dose rate estimates *J. Environ. Radioact.* **138** 249–63

[8] IAEA, Airborne Gamma Ray Spectrometer Surveying 1991 http://iaea.org/inis/collection/NCLCollectionStore/_Public/22/072/22072114.pdf (Accessed: 19 April 2018)

[9] Bucher B, Ludovic G, Strobel C, Butterweck G, Gutierrez S, Thomas M, Hohmann C, Krol I, Rybach L and Schwarz G 2009 *Int. Intercomparison Exercise of Airborne Gammaspectrometric Systems of Germany, France and Switzerland in the Framework of the Swiss Exercise—ARM07* http://iaea.org/inis/collection/NCLCollectionStore/_Public/41/030/41030200.pdf (Accessed: 28 May 2018)

[10] Guastaldi E *et al* 2013 A multivariate spatial interpolation of airborne γ-ray data using the geological constraints *Remote Sens. Environ.* **137** 1–11

[11] Sanada Y, Sugita T, Nishizawa Y, Kondo A and Torii T 2014 The aerial radiation monitoring in Japan after the Fukushima Daiichi nuclear power plant accident *Prog. Nucl. Sci. Technol.* **4** 76–80

[12] Sanada Y, Kondo A, Sugita T, Nishizawa Y, Youichi Y, Kazutaka I, Yasunori S and Torii T 2014 Radiation monitoring using an unmanned helicopter in the evacuation zone around the Fukushima Daiichi nuclear power plant *Explor. Geophys.* (Accessed: 3 February 2015) (https://doi.org/10.1071/EG13004)

[13] Towler J, Krawiec B and Kochersberger K 2012 Radiation mapping in post-disaster environments using an autonomous helicopter *Remote Sens.* **4** 1995–2015

[14] Martin P G, Payton O D, Fardoulis J S, Richards D A and Scott T B 2015 The use of unmanned aerial systems for the mapping of legacy uranium mines *J. Environ. Radioact.* **143** 135–40

[15] Martin P G, Payton O D, Yamashiki Y, Richards D A and Scott T B 2016 High-resolution radiation mapping to investigate FDNPP derived contaminant migration *J. Environ. Radioact.* **164** 26–35

[16] Safecast, About Safecast 2016 http://blog.safecast.org/about/

[17] Coletti M, Hultquist C, Kennedy W G and Cervone G 2017 Validating safecast data by comparisons to a US department of energy Fukushima prefecture aerial survey *J. Environ. Radioact.* **171** 9–20

[18] Tsuda S *et al* 2013 Construction of a car-borne survey system for measurement of dose rates in air, KURAMA-II, and its application (in Japanese) (https://doi.org/10.11484/JAEA-Technology-2013-037)

[19] Tsuda S, Yoshida T, Tsutsumi M and Saito K 2015 Characteristics and verification of a car-borne survey system for dose rates in air: KURAMA-II *J. Environ. Radioact.* **139** 260–5

[20] Buchanan E, Cresswell A J, Seitz B and Sanderson D C W 2016 Operator related attenuation effects in radiometric surveys *Radiat. Meas.* **86** 24–31

[21] Jones H E and Cunningham J R 1983 *Physics of Radiology* 4th edn (Springfield, IL: Thomas Publishing)

[22] Martin P G, Connor D, Payton O D, Leal-Olloqui M, Keatley A C and Scott T B 2018 Development and validation of a high-resolution mapping platform to aid in the public awareness of radiological hazards *J. Radiol. Prot.* **38** 329–42

[23] Grasty R, Kosanke K and Foote R 1979 Fields of view of airborne gamma-ray detectors *Geophysics* **44** 1447–57
[24] Pitkin J A and Duval J S 1980 Design parameters for aerial gamma ray surveys *Geophysics* **45** 1427–39
[25] Japanese Ministry of the Environment (Government of Japan) 2012 *Management of off-site Waste Contaminated with Radioactive Materials due to the Accident at Fukushima Nuclear Power Stations (Tokyo)* (https://env.go.jp/en/focus/docs/files/20121128-58.pdf)
[26] Watson P E, Watson I D and Bait R D 1980 Total body water volumes for adult males and females estimated from simple anthropometric measurements *Am. J. Clin. Nutr.* **33** 27–39
[27] Connor D T, Martin P G, Smith N T, Payne L, Hutton C, Payton O D, Yamashiki Y and Scott T B 2018 Application of airborne photogrammetry for the visualisation and assessment of contamination migration arising from a Fukushima waste storage facility *Environ. Pollut.* **234** 610–9
[28] Japan Meteorological Agency, Monthly total of precipitation (mm)—Japan Meteorological Agency, http://data.jma.go.jp/obd/stats/etrn/view/monthly_s3_en.php?block_no=47401&view=13 (Accessed: 14 January 2016)
[29] 2015 *CRC Handbook of Chemistry and Physics—Table of Isotopes* 96th edn (Boca Raton, FL: CRC Press) (http://hbcpnetbase.com/)